

Above- and below-threshold high-order-harmonic generation of H_2^+ in intense elliptically polarized laser fields

K. Nasiri Avanaki,¹ Dmitry A. Telnov,² and Shih-I Chu¹

¹*Department of Chemistry, University of Kansas, Lawrence, Kansas 66045, USA*

²*Department of Physics, St. Petersburg State University, St. Petersburg 198504, Russia*

(Received 10 June 2014; published 26 September 2014)

We present an *ab initio* three-dimensional precision calculation and analysis of high-order-harmonic generation (HHG) of the hydrogen molecular ion subject to intense elliptically polarized laser pulses by means of the time-dependent generalized pseudospectral method in two-center prolate spheroidal coordinates. The calculations are performed for the ground and first excited electronic states of H_2^+ at the equilibrium internuclear separation $R = 2$ a.u. as well as for the stretched molecule at $R = 7$ a.u. The spectral and temporal structures of the HHG signal are explored by means of the wavelet time-frequency analysis. Several aspects of ellipticity-dependent dynamical behaviors are uncovered. We found that the production of above-threshold harmonics for nonzero ellipticity is generally reduced, as compared with linearly polarized fields. However, below-threshold harmonics still appear quite strong except when the polarization plane is perpendicular to the molecular axis. Weak even harmonics are detected in the HHG spectra of stretched molecules. This effect can be explained by the broken inversion symmetry due to dynamic localization of the electron density near one of the nuclei. Multiphoton resonance and two-center interference effects are analyzed for the exploration of the quantum origin of the predicted HHG spectral and dynamical behavior.

DOI: [10.1103/PhysRevA.90.033425](https://doi.org/10.1103/PhysRevA.90.033425)

PACS number(s): 33.80.Rv, 42.65.Ky

I. INTRODUCTION

The study of the high-harmonic generation (HHG) dynamics and spectroscopy in intense laser fields is one of the topics in the forefront of ultrafast science and technology [1,2]. Most of the studies so far have been focused on the use of linearly polarized (LP) laser fields, where the semiclassical three-step model [3,4] can provide qualitative understanding of the underlying processes. The use of elliptically polarized (EP) laser fields opens access to a number of strong-field atomic, molecular, and optical (AMO) and chemical processes that are either hindered or not present under the linear polarization. Earlier study of the HHG spectrum in EP fields showed that the HHG yield is decreased with increasing ellipticity [5,6]. There have also been extensive studies of the polarization properties of HHG generated in atomic gases [7,8]. For the last decade, HHG has become the most important method for generating extreme ultraviolet (XUV) attosecond pulses from intense infrared lasers [2,9]. Since the HHG yield is sensitive to driving laser ellipticity, it has been found recently that the EP light can be used for the generation of isolated attosecond pulses via polarization gating [10]. The study of HHG in EP laser pulses is thus of considerable current interest both theoretically and experimentally [11,12]. For the molecular systems, the extra internuclear degree of freedom and the ellipticity of the laser field provide extra control parameters for laser-molecule interactions and introduce some interesting features in strong-field HHG processes. However, these extra degrees of freedom also pose considerable challenge for accurate theoretical and computational study.

In this paper, we perform a fully *ab initio* three-dimensional (3D) and accurate investigation of the effect of ellipticity on the HHG dynamics and spectroscopy of H_2^+ molecules below and above the ionization threshold. We show that the generation mechanism of HHG in EP light is considerably different from that in LP light. Further, in the EP case, particular attention

must be paid to follow closely the subtle electron dynamics on the subfemtosecond time scale and the delicate generation mechanism of HHG below and above the ionization threshold. The specific features of HHG in EP light are presented and their quantum origins are explored in details.

The organization of this paper is as follows. In Sec. II, we briefly describe the method that we use for solving the time-dependent Schrödinger equation in prolate spheroidal coordinates and discuss how we calculate the HHG spectra from the time-dependent wave function. In Sec. III, we present our results regarding HHG of the ground and first excited electronic states of H_2^+ in three different cases. The resonance and two-center interference effects in the HHG spectra are discussed in detail. Particular attention is paid to the exploration of the fine structures of spectral and time profiles of HHG which provide us with physical insights regarding the underlying mechanisms for harmonic generation in different energy regimes. Section IV contains concluding remarks.

II. THEORY AND NUMERICAL TECHNIQUES

The simplest diatomic molecule, hydrogen molecular ion H_2^+ , has been treated many times previously to study various multiphoton processes in strong laser fields but it still remains an important prototype system for the investigation of the elliptical field effects in HHG of diatomic molecules. In order to get high-precision electronic structure results with the use of only a modest number of grid points, we apply the two-center time-dependent generalized pseudospectral (TDGPS) scheme in prolate spheroidal coordinates for accurate and efficient treatment of the time-dependent Schrödinger equation (TDSE) for diatomic molecular systems. The methodology for the HHG calculation starts with solving TDSE in prolate spheroidal coordinates, which are convenient for describing two-center problems. Here we briefly outline the method.

Detailed numerical procedures can be found in Refs. [13,14]. The time-dependent electron wave function $\Psi(\mathbf{r},t)$ of H_2^+ at a fixed internuclear distance satisfies the TDSE (atomic units $\hbar = m = e = 1$ are used unless stated otherwise):

$$i \frac{\partial}{\partial t} \Psi(\mathbf{r},t) = [H_0(\mathbf{r}) + V_{\text{ext}}(\mathbf{r},t)] \Psi(\mathbf{r},t). \quad (1)$$

Here H_0 is the unperturbed electronic Hamiltonian:

$$H_0(\mathbf{r}) = -\frac{1}{2} \nabla^2 + U(\xi, \eta). \quad (2)$$

$U(\xi, \eta)$ being the Coulomb interaction with the nuclei (the charge of each center is unity),

$$U(\xi, \eta) = -\frac{2\xi}{a(\xi^2 - \eta^2)}. \quad (3)$$

Here a is a half internuclear separation; the nuclei are located at the points $-a$ and a on the z axis. The prolate spheroidal coordinates ξ , η , and φ are related to Cartesian coordinates x , y , and z as follows:

$$x = a\sqrt{(\xi^2 - 1)(1 - \eta^2)}\cos(\varphi), \quad (4)$$

$$y = a\sqrt{(\xi^2 - 1)(1 - \eta^2)}\sin(\varphi), \quad (5)$$

$$z = a\xi\eta \quad (1 \leq \xi < \infty, \quad -1 \leq \eta \leq 1). \quad (6)$$

The initial wave function represents an eigenstate and can be obtained by solving the unperturbed eigenvalue problem:

$$H_0\Psi(\xi, \eta, \varphi) = E\Psi(\xi, \eta, \varphi). \quad (7)$$

In Eq. (1), $V_{\text{ext}}(t)$ is the term due to the coupling to the external field. We assume that the laser field is EP in the x - z plane:

$$\mathbf{f}(t) = f_0(t) \left[\frac{\varepsilon}{\sqrt{1 + \varepsilon^2}} \hat{\mathbf{e}}_x \cos(\omega_0 t) + \frac{1}{\sqrt{1 + \varepsilon^2}} \hat{\mathbf{e}}_z \sin(\omega_0 t) \right]. \quad (8)$$

Here ε is the ellipticity parameter and ω_0 is the carrier frequency. Then using the dipole approximation and the length gauge, we can write the interaction potential $V_{\text{ext}}(\xi, \eta, t)$ in the following form:

$$V_{\text{ext}}(\mathbf{r}, t) = \mathbf{r} \cdot \mathbf{f}(t) = af_0(t) \left[\frac{\varepsilon}{\sqrt{1 + \varepsilon^2}} \sqrt{(\xi^2 - 1)(1 - \eta^2)} \times \cos(\varphi) \cos(\omega_0 t) + \frac{1}{\sqrt{1 + \varepsilon^2}} \xi\eta \sin(\omega_0 t) \right]. \quad (9)$$

In our calculations, we use the sine-squared pulse shape, and the function $f_0(t)$ can be written as follows:

$$f_0(t) = f_0 \sin^2 \left(\frac{\pi t}{NT} \right), \quad (10)$$

where f_0 is the peak field strength, $T = 2\pi/\omega_0$ is the duration of one optical cycle, and N is the number of optical cycles in the pulse.

Since H_0 has a rotational symmetry with respect to the molecular axis, the unperturbed initial wave function can be written as

$$\Psi(\xi, \eta, \varphi) = \psi_m(\xi, \eta) \exp(im\varphi), \quad (11)$$

where m is the projection of the electron orbital angular momentum onto the molecular axis. The generalized pseudospectral method [14,15] is employed to discretize ξ, η and propagate the time-dependent wave function in the energy representation using the second-order split-operator method according to

$$\begin{aligned} \Psi(\mathbf{r}, t + \Delta t) \approx & \exp \left[-i \frac{\Delta t}{2} H_0(\mathbf{r}) \right] \\ & \times \exp \left[-i \Delta t V \left(\xi, \eta, t + \frac{1}{2} \Delta t \right) \right] \\ & \times \exp \left[-i \frac{\Delta t}{2} H_0(\mathbf{r}) \right] \Psi(\mathbf{r}, t) + O(\Delta t^3). \end{aligned} \quad (12)$$

Once the wave function is computed, we can proceed to calculate the spectra of the emitted high-order-harmonic radiation. To calculate the HHG spectra, we employ the widely used semiclassical approach, replacing the classical quantities with the corresponding quantum expectation values. The spectral density of the radiation energy emitted for all the time is given either by the length form,

$$S(\omega) = \frac{2\omega^4}{3\pi c^3} |\mathbf{D}_\omega|^2, \quad (13)$$

or acceleration form,

$$S(\omega) = \frac{2}{3\pi c^3} |\mathbf{A}_\omega|^2. \quad (14)$$

\mathbf{D}_ω and \mathbf{A}_ω are the Fourier transforms of the time-dependent dipole moment and acceleration, respectively:

$$\mathbf{D}_\omega = \int_{-\infty}^{\infty} dt \mathbf{D}(t) \exp(i\omega t), \quad (15)$$

$$\mathbf{A}_\omega = \int_{-\infty}^{\infty} dt \mathbf{A}(t) \exp(i\omega t). \quad (16)$$

The time-dependent dipole moment and acceleration are evaluated as expectation values with the time-dependent wave function $\Psi(\xi, \eta, \varphi, t)$:

$$\mathbf{D}(t) = \langle \Psi | \mathbf{r} | \Psi \rangle, \quad (17)$$

$$\mathbf{A}(t) = -\langle \Psi | \nabla U | \Psi \rangle - \mathbf{f}(t). \quad (18)$$

By adjusting the numerical parameters of the present calculations, such as the number of grid points, the box size, and absorber position, we reproduce the ground state and low-lying excited states' energies of H_2^+ with machine accuracy. To achieve convergence of the computed HHG spectra for the laser field parameters and internuclear separations used in the calculations (see Sec. III), we set the number of grid points to 160 and 48 for the ξ and η coordinates, respectively, and include the angular momentum projections -24 to 24 . For the time propagation, we use 4096 time steps per optical cycle (81 920 steps for the whole pulse of 20 optical cycles). To accommodate all important physics in the laser field, the linear dimension of the box is chosen at 60 a.u. In the layer between 40 and 60 a.u., we place an absorber which prevents spurious reflections of the wave packet from the grid boundary.

Our numerical scheme and selection of the parameters secure the accuracy of the results obtained. In the calculations of the HHG spectra, we use the length form (15); the acceleration form provides almost identical results, indicating the good quality of our wave functions.

III. RESULTS AND DISCUSSION

We have performed the calculations of HHG spectra emitted by H_2^+ in $1\sigma_g$ and $1\sigma_u$ electronic states in an intense EP laser field. In all cases we used a 20-optical-cycles laser pulse with the sine-squared envelope, the carrier wavelength 800 nm (corresponding to the photon energy 1.55 eV), and the peak intensity 2×10^{14} W/cm². According to the well-known atomic recollision model [3], the HHG spectra should present a plateau region with a cutoff at the energy $|I_P| + 3.17U_P$ where $|I_P|$ is the ionization energy of the initial state and U_P is the ponderomotive potential [for the LP laser field, $U_P = I^2/(4\omega_0^2)$, I being the laser intensity]. For diatomic molecules, the collision with the parent core resembles the single-atom case and leads to the same harmonic spectrum cutoff position independent of the laser field intensity and internuclear separation. However, there is a possibility of collision with the other nucleus. In the latter case, the field intensity and frequency as well as the distance between the nuclei can affect the return kinetic energy of the electron [16]. The vertical ionization potential I_P of H_2^+ is equal to 30 eV for the $1\sigma_g$ state and 18 eV for the $1\sigma_u$ state, at the equilibrium internuclear separation of 2 a.u. Then the cutoff corresponds to the harmonic orders 43 and 36, respectively.

A. HHG spectra of H_2^+ in $1\sigma_g$ electronic state

Figure 1(a) shows the HHG spectral density of H_2^+ for $1\sigma_g$ electronic state with different ellipticity parameters. As one can see, the semiclassically predicted cutoff positions are in fair agreement with our calculations in the LP field.

Generally, elliptical polarization (and circular polarization to a greater extent) will reduce the probability of recollision and thus reduce the intensity of above-threshold harmonics (that is, harmonics with the photon energies above the ionization threshold). The intensity of below-threshold harmonics (harmonics with the photon energies below the ionization threshold) is also reduced because the dipole transitions are forbidden if the angular momentum projection m is changed by more than unity (and each absorbed circularly polarized photon increases m by 1). All this is true for atoms in laser fields. For molecules, the picture is different: first, due to broken spherical symmetry and the m selection rule; second, because the recollision can take place not only on the parent nucleus but also on the other nucleus. Our results demonstrate specific differences between the atoms and molecules. As expected, the HHG cutoff position is shifted to lower frequencies as the ellipticity parameter increases from 0 (linear polarization) to 1 (circular polarization). Interestingly, just a few of the lower harmonics show up in the circularly polarized (CP) field. Comparing the intensity of the harmonics in different cases ($\varepsilon = 0, 0.5, 1$) presented in Fig. 1(a), we can see that the intensities of lower-order harmonics are comparable. However, as we go to higher harmonics, their intensities in the EP and CP fields decrease by several orders of magnitude with respect to the linear polarization case. Looking carefully at Fig. 1(b), one can notice the peaks at the harmonic orders 7.65 and 11.65, which do not correspond to odd integer numbers. Based on the unperturbed electronic energy values of H_2^+ , we attribute the first peak, located near the seventh harmonic (harmonic order 7.65), to the resonance with the first excited ($1\sigma_u$) state. Accordingly, the second peak, which appears close to the 11th harmonic (harmonic order 11.65), is attributed to the resonance with the second excited ($1\pi_u$) state. We note that the first resonance peak shows up in the HHG spectrum irrespectively of the ellipticity parameter, while the second resonance is absent in the linear polarization case ($\varepsilon = 0$). This is well explained by the dipole selection rules: Transitions between σ

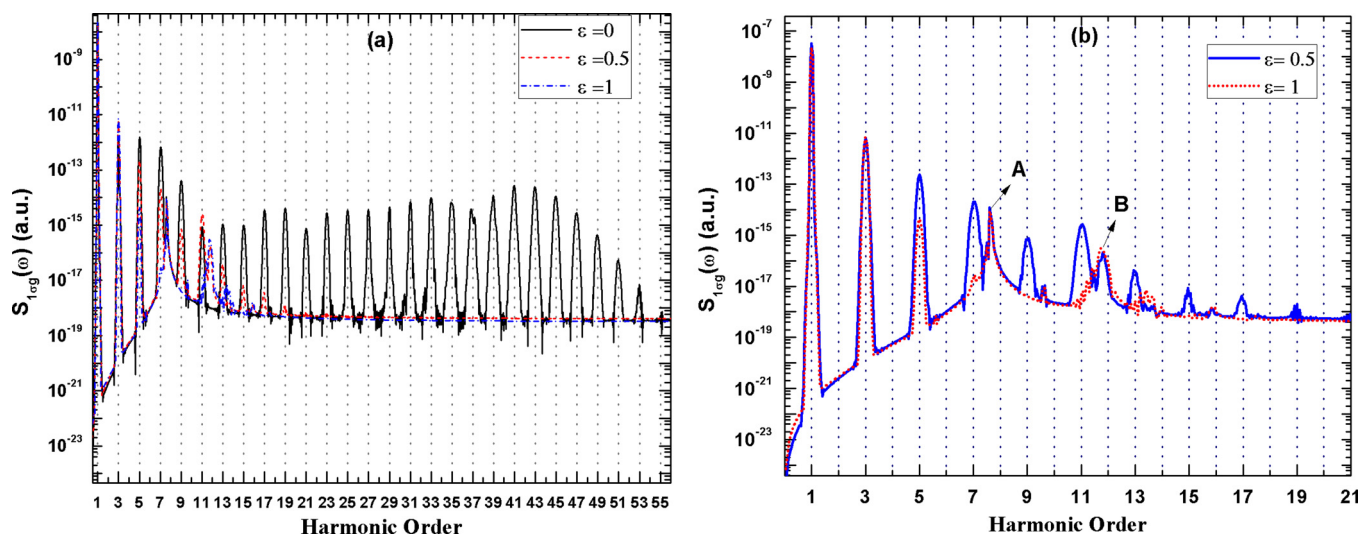


FIG. 1. (Color online) (a) HHG spectrum $S(\omega)$ from $1\sigma_g$ state of H_2^+ at $R = 2$ a.u. in the laser field with $\lambda = 800$ nm and peak intensity 2×10^{14} W/cm² for different ellipticity parameters ($\varepsilon = 0, 0.5, 1$). (b) Resonance structures for ($\varepsilon = 0.5, 1$) near the seventh and 11th harmonics. Arrows mark the resonance peaks in the spectrum in CP field. Resonance A corresponds to excitation of $1\sigma_u$ state, resonance B is due to coupling to $1\pi_u$ state.

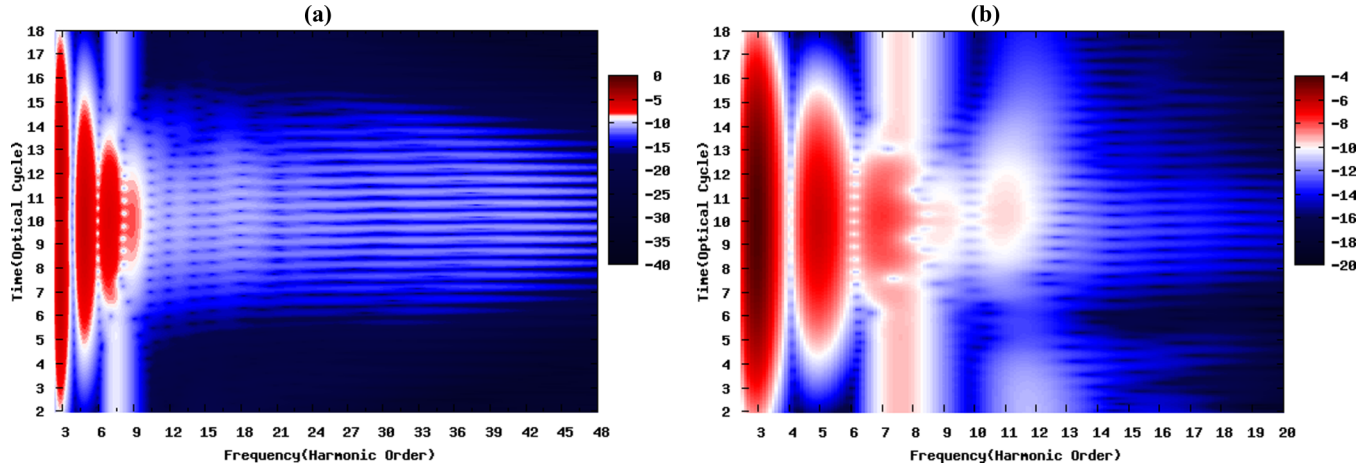


FIG. 2. (Color online) Time-frequency spectra for $1\sigma_g$ state of H_2^+ at $R = 2$ a.u. in the field with $\lambda = 800$ nm and peak intensity 2×10^{14} W/cm 2 for different ellipticity parameters $\varepsilon = 0$ in (a) and $\varepsilon = 0.5$ in (b). The color scale is logarithmic.

and π states are forbidden when the external field is directed along the molecular axis.

To explore the detailed spectral and temporal structure of HHG and the underlying mechanisms in different regimes, we perform the time-frequency analysis by means of the wavelet transform [17,18] of the induced dipole,

$$d_\omega(t_0) = \int D(t)W_{t_0,\omega}(t)dt, \quad (19)$$

with the wavelet kernel $W_{t_0,\omega}(t) = \sqrt{\omega}W[\omega(t - t_0)]$. For the harmonic emission, a natural choice of the mother wavelet is given by the Morlet wavelet [18]:

$$W(x) = \left(\frac{1}{\sqrt{\tau}}\right)e^{ix} \exp\left(\frac{-x^2}{2\tau^2}\right). \quad (20)$$

Here the wavelet window function varies with the frequency but the total number of oscillations (proportional to τ) within the window is fixed; however, in the Gabor transform [18] the width of the window function is held constant. For the calculations discussed below, we choose $\tau = 15$ to perform the wavelet transform.

In Figs. 2(a) and 2(b), we show the absolute value of the time-frequency spectrum $|d_\omega(t)|$ for the $1\sigma_g$ state of H_2^+ at $R = 2$ a.u. in laser fields with peak intensity 2×10^{14} W/cm 2 and ellipticity parameters ($\varepsilon = 0$) and ($\varepsilon = 0.5$). The $1\sigma_u$ resonance is clearly seen at the harmonic order 7.65 in both LP and EP fields, while the $1\pi_u$ resonance shows up at the harmonic order 11.65 in the case of elliptical polarization only.

The cross section of the time-frequency profile corresponding to a specific harmonic order yields a function of time which exhibits a different pattern depending on the harmonic order. For the lowest few harmonics and all ellipticities that we study here, we obtain a smooth function, which resembles the envelope of the driving laser pulse. This is a manifestation of the dominant multiphoton mechanism in the lower-harmonic regime. In this regime, the probability of absorbing N photons is about I^N (I is the laser intensity and proportional to $[f(t)]^2$). In this part of the HHG spectrum, the smooth time profile becomes narrower as the harmonic order is increased. In the frequency domain, the corresponding frequency profile

becomes wider (see Fig. 2). As the harmonic order is further increased in the below-threshold region, the time profiles develop spread fine structures, which resemble the pattern for the above-threshold harmonics and may be attributed to the effect of the quasicontinuum formed by highly excited bound states.

For higher harmonics above the ionization threshold, the time profiles manifest multiple bursts, with two bursts per optical cycle. Each burst is due to the recollision of the electronic wave packet with the ionic core. Transformation of the time-frequency spectra with increasing harmonic order is well illustrated by Fig. 2.

One can see that the (multiphoton-dominant) low-order harmonics form *continuous time profiles* at a given frequency. However, for higher-harmonic orders, the tunneling-recollision mechanism becomes dominant, and the time-frequency profiles show a netlike structure. This structure is more pronounced for the LP field [Fig. 2(a)] than in the case of elliptical polarization [Fig. 2(b)]. This is well understood since the recollision becomes increasingly suppressed when the ellipticity parameter increases.

We have also performed calculations on stretched H_2^+ molecules with the internuclear separation $R = 7$ a.u. The HHG spectra $S(\omega)$ are shown in Figs. 3(a) and 3(b). The two lowest electronic states, $1\sigma_g$ and $1\sigma_u$, become nearly degenerate at larger R (at $R = 7$ a.u., their vertical ionization potentials are 17.6 and 17.4 eV, respectively). In the presence of the external fields, the electric dipole coupling of $1\sigma_g$ and $1\sigma_u$ is proportional to R and becomes very significant. This phenomenon, known as the “charge resonance” (CR) effect, takes place only in the odd-charged molecular-ion systems. In LP fields, the combined effect of CR and the multiphoton transitions to excited electronic states is the main mechanism responsible for the enhanced ionization phenomenon [13]. Compared with the case $R = 2$ a.u., the ionization probability of H_2^+ is greatly increased due to reduced ionization potential in stretched molecules at $R = 7$ a.u. (the minimum number of photons required for ionization of the $1\sigma_g$ state is equal to 11, compared to 20 at $R = 2$ a.u.). According to the three-step model [16], it leads to enhancement in HHG, resulting in more intense signal and appearance of more distinct harmonics in the high-energy region of the spectrum [see Fig. 3(b)].

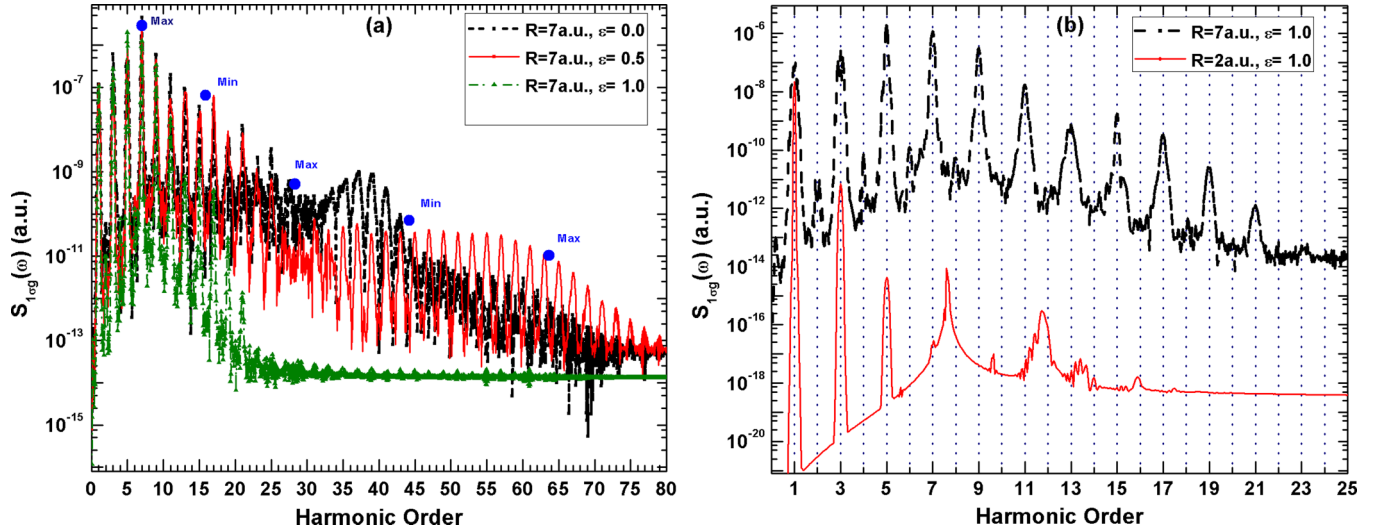


FIG. 3. (Color online) HHG spectra $S(\omega)$ from $1\sigma_g$ state of H_2^+ at $R = 7$ a.u. in the laser field with $\lambda = 800$ nm and peak intensity 2×10^{14} W/cm 2 . (a) HHG spectra for different ellipticity parameters ($\epsilon = 0.5, 1$). (b) Comparison of HHG spectra for the same laser field parameters for CP at $R = 7$ a.u. and $R = 2$ a.u.

The HHG spectra in Fig. 3(a) for LP and EP fields exhibit several maxima and minima that can be related to the two-center nature of diatomic molecules [19] (see also discussion in Refs. [14,20]). Since the returning electron can experience a recollision at any nucleus, the contributions to the recombination amplitude from both nuclei are added coherently, giving rise to the interference structure in the HHG spectra. Using a simple recollision model, one can easily obtain the interference minima or maxima positions in the case of LP fields [19]:

$$\cos\alpha = \frac{n\pi}{R\sqrt{2E_{ke}}} \quad n = 1, 2, 3, \dots, \quad (21)$$

where E_{ke} is the kinetic energy of the recolliding electron, α is the angle between the polarization vector of the laser field and the molecular axis, and R is the distance between the two centers (that is, internuclear distance for diatomic molecules).

Assuming all the kinetic energy of the electron is transformed into the harmonic radiation energy during the recollision ($E_{ke} = N_h\omega_0$, where N_h is the harmonic order), for the laser field parallel to the molecular axis ($\cos\alpha = 1$), and for the given internuclear separation R and laser frequency ω_0 , one can obtain the harmonic order N_h where the minimum or maximum should be located. For the $1\sigma_g$ state, $n = 1, 3, 5, \dots$ in Eq. (21) correspond to a minimum, and $n = 2, 4, 6, \dots$ correspond to a maximum. Thus a simple calculation can give us an estimate of the harmonic order where the interference maxima or minima are expected in the HHG spectrum. For H_2^+ at the internuclear separation $R = 7$ a.u. subject to the 800-nm LP laser field, only the first few minima and maxima can be relevant for the two-center interference analysis of the HHG spectrum. For $n = 3$ and $n = 5$, the minima can be expected at the harmonic orders 16 and 44, respectively. The maxima for $n = 2, 4, 6$ can be found around the harmonic orders 7, 28, and 63. These positions are marked in Fig. 3(a) with blue circles. Except for the maximum at the harmonic order 28, the other predictions are in fair agreement with our calculations. We should note that Eq. (21) represents a rough model and

is derived in the case of linear polarization; for EP fields, the estimates based on this equation become even less accurate.

At the internuclear separation $R = 7$ a.u., a comb of well-resolved odd- and even-order harmonics, particularly in the lower-energy part of the HHG spectra, is observed. The odd harmonics are at least four orders of magnitude stronger than the even harmonics [see Fig. 3(b) where the spectra at $R = 2$ a.u. and $R = 7$ a.u. are compared in the case of CP field]. By varying numerical simulation parameters such as the number of grid points, the box size, and the absorber position, we have confirmed that the results are converged and the existence of even harmonics cannot be attributed to numerical inaccuracy. This is surprising since one would not normally expect generation of even harmonics from homonuclear diatomic molecules. Generally, generation of even harmonics is forbidden by a fundamental symmetry, which combines the inversion symmetry of the media and the half-wave symmetry of the driving field. Thus in atoms, the presence of only odd harmonics is an indication of the spatial inversion symmetry of the electron-atom interaction energy [21,22]; the same is true for homonuclear diatomic molecules. It is proven that if *heteronuclear* diatomic molecules in the gas are oriented [23] or if the half-wave symmetry of the driving field is broken [24], then the HHG spectrum consists of both odd and even harmonics. Strictly speaking, if the driving field represents a pulse but not a continuous wave, the half-wave symmetry is broken, and generation of even harmonics is possible. However, this effect is negligible for long enough pulses. Indeed, for the pulse duration of 20 optical cycles, we do not see even harmonics at the internuclear distance $R = 2$ a.u., but those harmonics do appear at $R = 7$ a.u. We explain this phenomenon by the effect of a dynamical rupture of symmetry (DRS) [25,26]. The idea behind DRS is that the electron, initially symmetrically distributed over the two nuclei, becomes essentially localized over one of the nuclei, and periodically bounces back and forth from nucleus to nucleus. During the confinement time over one of the two nuclei, the electron experiences a nonsymmetric potential,

which is the sum of the symmetric atomic potential of the near nucleus plus the tail of the potential of the far nucleus; this DRS causes the emission of even harmonics [25,26]. For H_2^+ at the internuclear separation $R = 7$ a.u., the DRS effect is enhanced by the existence of the CR states. In the laser field with the intensity as high as 2×10^{14} W/cm², a significant amount of the electron population is transferred from the initial $1\sigma_g$ state to the $1\sigma_u$ state, resulting in a nonsymmetric electron density distribution.

B. HHG spectra of H_2^+ in $1\sigma_u$ electronic state

We have also performed the calculations of the HHG spectra emitted by H_2^+ in the $1\sigma_u$ (first excited) electronic state. The parameters of the laser pulse are the same as in the previous calculations at $R = 2$ a.u. Figure 4(a) displays the HHG spectra of H_2^+ for the $1\sigma_u$ electronic state with different ellipticity parameters $\varepsilon = 0, 0.5, 1$. We can see that the HHG cutoffs are shifted to lower energies as the ellipticity parameter increases from linear to circular polarization, in agreement with general predictions for EP laser fields. It appears that the HHG signal for the initial $1\sigma_u$ state is several orders of magnitude stronger than that for the $1\sigma_g$ state, with the same laser pulse parameters, as one can see from Figs. 4(a) and 4(b). This is well explained by much lower ionization potential (and, hence, much higher ionization probability) of the $1\sigma_u$ state at the internuclear separation $R = 2$ a.u. Analysis of below-threshold harmonics (the minimum number of photons required for ionization is 12 while the cutoff is around harmonic order 36) in the cases $\varepsilon = 0.5$ and $\varepsilon = 1$ [Fig. 4(b)] reveals resonance peaks in the vicinity of the fifth and seventh harmonics. The unperturbed bound-state energies of H_2^+ suggest that the first peak, which appears near the fifth harmonic, corresponds to the resonance with the $2\sigma_g$ state. As to the second peak, located near the seventh harmonic, it can be attributed to the resonances with the $1\sigma_g$, $3\sigma_g$, and $1\pi_g$ states. These resonances are not resolved

into separate peaks since their transition energies are very close to each other.

Since the diatomic molecule H_2^+ does not possess spherical symmetry, the effect of the EP laser field depends on the orientation of the molecular axis with respect to the polarization plane of the field. Above we have studied one representative case, when the molecular axis lies in the polarization plane and is directed along the major axis of the polarization ellipse. Now we consider another important case, when the molecular axis is perpendicular to the polarization plane (that is, the field is polarized in the x - y plane):

$$\mathbf{f} = f_0(t) \left[\frac{\varepsilon}{\sqrt{1+\varepsilon^2}} \hat{e}_x \cos(\omega_0 t) + \frac{1}{\sqrt{1+\varepsilon^2}} \hat{e}_y \sin(\omega_0 t) \right], \quad (22)$$

$$\begin{aligned} V_{\text{ext}}(t) = \mathbf{r} \cdot \mathbf{f} &= a f_0 \sin^2 \left(\frac{\pi t}{nT} \right) \sqrt{(\xi^2 - 1)(1 - \eta^2)} \\ &\times \left[\frac{\varepsilon}{\sqrt{1+\varepsilon^2}} \cos(\varphi) \cos(\omega_0 t) \right. \\ &\left. + \frac{1}{\sqrt{1+\varepsilon^2}} \sin(\varphi) \sin(\omega_0 t) \right]. \quad (23) \end{aligned}$$

Here we report the results regarding the circular polarization ($\varepsilon = 1$) only. For the polarization in the x - y plane, the situation resembles the atomic case since the same selection rules apply to the angular momentum projection onto the axis perpendicular to the polarization plane (that is, the molecular axis). For the unperturbed molecule, the angular momentum projection m on the molecular (z) axis is conserved. In the CP field in the x - y plane, absorption of each photon changes this projection by $\Delta m = 1$ or $\Delta m = -1$ for the right and left polarization, respectively. Thus absorption of several photons from the field leads to population of the states with large m values; dipole transitions from such states to the ground state

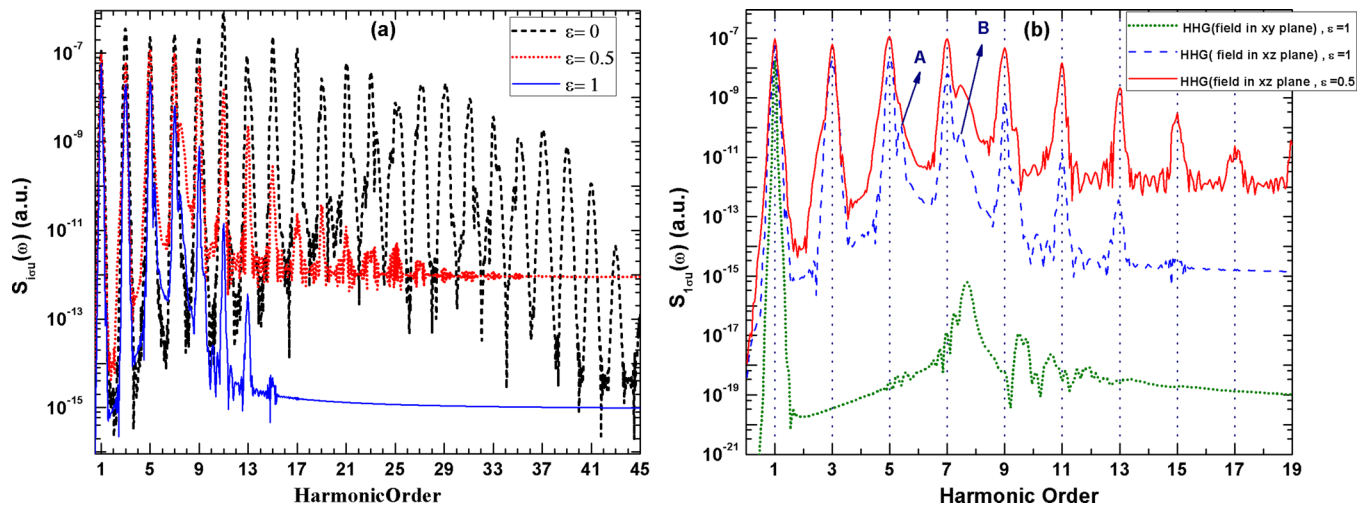


FIG. 4. (Color online) HHG spectra $S(\omega)$ from $1\sigma_u$ state of H_2^+ at $R = 2$ a.u. in the laser field with $\lambda = 800$ nm and peak intensity 2×10^{14} W/cm². (a) HHG spectra for the field polarized in the x - z plane and ($\varepsilon = 0, 0.5, 1$). (b) HHG spectra for $\varepsilon = 0.5, 1$ with resonance structures near the fifth and seventh harmonics. The arrows mark the resonance peaks in the spectrum. Resonance A corresponds to excitation of $2\sigma_g$ state; resonance B is due to coupling to $1\sigma_g$, $3\sigma_g$, and $1\pi_g$ states. Also shown is the HHG spectrum for the CP field in the x - y plane.

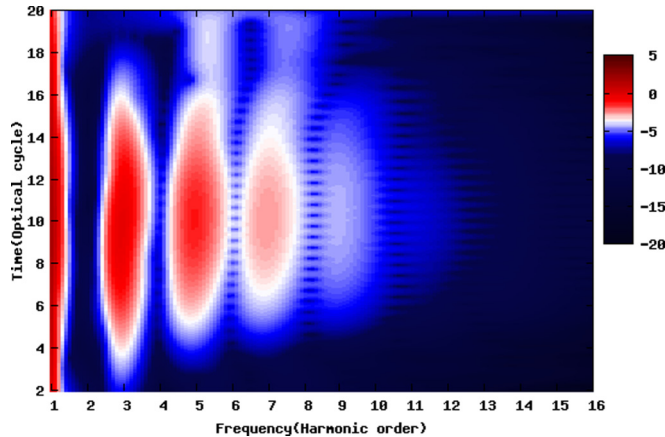


FIG. 5. (Color online) Time-frequency spectra for $1\sigma_u$ state of H_2^+ at $R = 2$ a.u. in the field with $\lambda = 800$ nm, peak intensity 2×10^{14} W/cm 2 , and the ellipticity parameter $\varepsilon = 1$. The color scale is logarithmic.

with emission of a single photon are forbidden by the selection rules. In Fig. 4(b), we can see strong suppression of HHG for both below-threshold and above-threshold harmonics. For the polarization in the x - z plane, the situation is different: The HHG is suppressed but not as much as in the x - y polarization case. Moreover, the below-threshold harmonics are quite strong, and this happens because there is no $\Delta m = \pm 1$ selection rule (for each absorbed photon) with respect to the molecular axis.

To illustrate the mechanisms of HHG in the $1\sigma_u$ state of H_2^+ , we perform a time-frequency analysis and plot the time-frequency spectrum $|d_\omega(t)|$ for the case of circular polarization in the x - z plane (Fig. 5). One can clearly see the resonances near the fifth and seventh harmonics; the resonance lines remain quite strong even at the end of the pulse, when the external field vanishes. The HHG mechanisms are revealed by the time profiles of the harmonics in different energy regions obtained by performing the cross section of the time-frequency spectrum. For the lowest few harmonics, the time profile (at a given frequency) shows a smooth function corresponding to the envelope of the driving laser pulse. This behavior resembles what we obtain for the $1\sigma_g$ state and manifests the dominant multiphoton mechanism in the low-energy region.

Development of extended fine structures in the time profiles of the higher-harmonic order can be attributed to the effect of excited states and the onset of the continuum. In the intermediate energy regime, where both multiphoton and tunneling mechanisms contribute, the time-frequency profiles show a netlike structure, as seen in Fig. 5. Since the HHG spectrum in the circular polarization case is quite short, and there is no clear plateau well above the ionization threshold, the fast burst time profiles corresponding to the tunneling regime are developed by a few harmonics only.

IV. CONCLUSION

In conclusion, we have presented an *ab initio* high-precision study of high-order-harmonic generation of the hydrogen molecular ion in intense laser fields. It is found that the HHG yield is very sensitive to the ellipticity of the driving laser field. The reduction in the production of above-threshold harmonics for nonzero ellipticity, particularly for $\varepsilon = 0.5$ and $\varepsilon = 1$, is partially explained by the third step of the recollision model: The transverse component of the laser field tilts the trajectory of the electron and prevents it from recombining with the parent nucleus (it may recombine with the other nucleus, however). If the polarization plane of the laser field contains the molecular axis, the below-threshold harmonics still appear quite strong, even for circular polarization, in contrast with the case when the polarization plane is perpendicular to the molecular axis. This happens because the excited bound states with the angular momentum projections $m = 0$ and $m = 1$ onto the molecular axis (that is, σ and π states) still can be populated by absorption of multiple photons in the CP field, provided the molecular axis has a nonzero projection in the polarization plane. These excited states then allow transitions to the ground state with emission of a single photon.

Such multiphoton excitations followed by transitions to the ground state with emission of a single photon are not permitted for atoms since atomic states possess definite angular momentum, which must increase by one after absorption of each CP photon. Thus the reduced symmetry of diatomic molecules, as compared with atoms, leads to qualitative differences between the atomic and molecular HHG spectra in EP laser fields, with higher HHG yield from molecules. Another feature revealed by the present calculations is also related to the reduced symmetry. Weak even harmonics observed in the HHG spectra of H_2^+ molecules stretched at the internuclear distance $R = 7$ a.u. can be explained by dynamically broken inversion symmetry, when the electron density is periodically localized near one of the two nuclei.

The method discussed in the present paper for the one-electron molecular ion H_2^+ can be generalized for multielectron diatomic molecules with the help of the self-interaction-free time-dependent density functional theory [20,27,28]. For multielectron molecules, commonly used restriction to the highest-occupied molecular orbital may appear insufficient. Correct description of the HHG spectra in this case may require taking into account the inner-shell orbitals as well. Extension of the time-dependent density functional theory (TDDFT) for the study of HHG from multielectron diatomic molecules in EP laser fields is in progress.

ACKNOWLEDGMENTS

This work is partially supported by the Chemical Sciences, Geosciences and Biosciences Division of the Office of Basic Energy Sciences, Office of Sciences, US Department of Energy. D.A.T. acknowledges the partial support of St. Petersburg State University (Grant No. 11.38.654.2013).

[1] S. R. Leone *et al.*, *Nat. Photon.* **8**, 162 (2014).

[2] Z. Chang and P. Corkum, *J. Opt. Soc. Am. B* **27**, B9 (2010).

[3] P. B. Corkum, *Phys. Rev. Lett.* **71**, 1994 (1993).

[4] K. C. Kulander, K. J. Schafer, and J. L. Krause, in *Super-Intense Laser-Atom Physics*, edited by B. Piraux, A. L'Huillier, and

- K. Rzażewski, NATO Advanced Study Institute Series B: Physics, Vol. 316 (Plenum, New York, 1993).
- [5] K. S. Budil, P. Salières, A. L’Huillier, T. Ditmire, and M. D. Perry, *Phys. Rev. A* **48**, R3437 (1993).
- [6] Y. Liang, M. V. Ammosov, and S. L. Chin, *J. Phys. B* **27**, 1269 (1994).
- [7] J. G. Eden, *Prog. Quantum Electron.* **28**, 197 (2004); **29**, 257(E) (2005).
- [8] D. B. Milošević, W. Becker, and R. Kopold, *Phys. Rev. A* **61**, 063403 (2000).
- [9] F. Krausz and M. Ivanov, *Rev. Mod. Phys.* **81**, 163 (2009).
- [10] M. Möller, Y. Cheng, S. D. Khan, B. Zhao, K. Zhao, M. Chini, G. G. Paulus, and Z. Chang, *Phys. Rev. A* **86**, 011401 (2012).
- [11] S. D. Khan, Y. Cheng, M. Möller, K. Zhao, B. Zhao, M. Chini, G. G. Paulus, and Z. Chang, *Appl. Phys. Lett.* **99**, 161106 (2011).
- [12] M. V. Frolov, N. L. Manakov, T. S. Sarantseva, and A. F. Starace, *Phys. Rev. A* **86**, 063406 (2012).
- [13] X. Chu and Shih-I Chu, *Phys. Rev. A* **63**, 013414 (2000).
- [14] D. A. Telnov and Shih-I Chu, *Phys. Rev. A* **76**, 043412 (2007).
- [15] X.-M. Tong and Shih-I Chu, *Chem. Phys.* **217**, 119 (1997).
- [16] R. Kopold, W. Becker, and M. Kleber, *Phys. Rev. A* **58**, 4022 (1998).
- [17] X.-M. Tong and Shih-I Chu, *Phys. Rev. A* **61**, 021802(R) (2000).
- [18] C. K. Chui, *An Introduction to Wavelets* (Academic Press, New York, 1992).
- [19] M. Lein, N. Hay, R. Velotta, J. P. Marangos, and P. L. Knight, *Phys. Rev. A* **66**, 023805 (2002).
- [20] D. A. Telnov and S. I. Chu, *Phys. Rev. A* **80**, 043412 (2009).
- [21] M. H. Mittleman, *Theory of Laser Atom Interaction* (Plenum, New York, 1982).
- [22] F. Martín, J. Fernández, T. Havermeier, L. Foucar, Th. Weber, K. Kreidi, M. Schöffler, L. Schmidt, T. Jahnke, O. Jagutzki, A. Czasch, E. P. Benis, T. Osipov, A. L. Landers, A. Belkacem, M. H. Prior, H. Schmidt-Böcking, C. L. Cocke, and R. Dörner, *Science* **315**, 629 (2007).
- [23] E. Frumker, C. T. Hebeisen, N. Kajumba, J. B. Bertrand, H. J. Worner, M. Spanner, D. M. Villeneuve, A. Naumov, and P. B. Corkum, *Phys. Rev. Lett.* **109**, 113901 (2012).
- [24] M. Kozlov, O. Kfir, A. Fleischer, A. Kaplan, T. Carmon, H. G. L. Schwefel, G. Bartal, and O. Cohen, *New J. Phys.* **14**, 063036 (2012).
- [25] G. Castiglia, P. P. Corso, R. Daniele, E. Fiordilino, F. Morales, and G. Orlando, *Laser Phys.* **17**, 1240 (2007).
- [26] P. P. Corso, E. Fiordilino, G. Orlando, and F. Persico, *J. Mod. Optics* **54**, 1387 (2007).
- [27] X. Chu and Shih-I Chu, *Phys. Rev. A* **63**, 023411 (2001).
- [28] J. Heslar, D. Telnov, and Shih-I Chu, *Phys. Rev. A* **83**, 043414 (2011).